

Towards predicting temporal changes of the spectral signature of snow in visible and near-infrared wavelengths

ROBERT E. DAVIS

U.S. Army Cold Regions Research and Engineering Laboratory, 72 Lyme Road, Hanover, NH 03755-1290, U.S.A.

ANNE W. NOLIN

Center for Remote Sensing and Environmental Optics, University of California Santa Barbara, Santa Barbara, CA 93106, U.S.A.

RACHEL JORDAN

U.S. Army Cold Regions Research and Engineering Laboratory, 72 Lyme Road, Hanover, NH 03755, U.S.A.

JEFF DOZIER

Center for Remote Sensing and Environmental Optics, University of California Santa Barbara, Santa Barbara, CA 93106, U.S.A.

ABSTRACT. This study links two models, one that simulates changes in snow microstructure and one that recovers microstructure properties from measurements of snow reflectance. An energy and mass transfer model, SN THERM.89, was used to calculate snow grain growth. Grain-sizes from the model and measurements of grain bond areas provided estimates of the surface-to-volume ratio of the bulk snow, which were transformed to geometrically-equivalent sphere sizes. An inversion technique based on a discrete-ordinate model of the directional reflectance recovered optically-equivalent sphere sizes from reflectance measurements at 1.075 μm . The predictions of equivalent sphere sizes from the snow model and the recovered optical sphere sizes from the inversion method were compared with stereological measurements from snow sections. The geometrically-equivalent and optically-equivalent grain-sizes showed good agreement with each other and with stereological measurements from snow a few days old. The predictions of the reflectance inversion method also compared favorably with geometrically-equivalent grain-sizes measured from a melt-freeze surface crust. This investigation showed the potential for fully coupling snow property simulations with models to predict the spectral reflectance of snow.

INTRODUCTION

This research explores the potential to couple fully an energy balance model to a model of the directional reflectance of snow. Spectral transmission and absorption of solar radiation in a snow cover is not fully understood, and the volume heating effects play important roles in snow metamorphism and melting. In addition, efforts are currently under way to distribute energy balance models over complex terrain. One viable method to validate algorithms that distribute point energy balance models is by recovering snow properties from remote sensing data. To do this requires that the snow property simulations and recovery algorithms use the same parameters. In this regard, we examine the optically-equivalent sphere used to model reflectance in the solar spectrum.

The snowpack radiation balance controls heating and melting in the surface layer of snow, which affects the spectral reflectance. In the near-infrared wavelengths, snow reflectance depends on the specific surface area of the ice matrix while, in the visible spectral region,

reflectance is controlled by the amounts and distributions of absorbing impurities (Warren and Wiscombe, 1980; Wiscombe and Warren, 1980). The specific surface of the snow matrix depends on the metamorphic state of the snow. Radiation is often the dominant component of the energy budget and in dry snow it exerts strong control on the temperature profiles near the snow-atmosphere interface. This in turn drives snow metamorphism, leading to changes in snow grain size and reflectance (Colbeck 1989). When snow is initially wetted, grain growth proceeds rapidly depending on the liquid water content. Moreover, grain clusters form quickly (Colbeck, 1979), which dramatically reduces the pore surface area (Davis, 1991) and in turn reduces the snow reflectance (Grenfell and Maykut, 1977).

APPROACH

In this work, a one-dimensional model of the energy and mass budget of a snow cover was used to predict the

growth of snow grains, the compaction rate and densification of the snow, and the liquid water content. The fraction of the ice grain-to-grain contact surface occupied by bonds is not calculated by the model, so measurements were made of bond lines. Predicted grain sizes and estimates of the total fractional area of grain contacts were used to calculate the surface-to-volume ratio of the ice matrix, which was converted to the geometrically-equivalent sphere size. The sphere with the same surface-to-volume ratio as the bonded ice grains, has been used as the "optically-equivalent" grain for modeling snow reflectance in the visible and near-infrared spectral region (Dozier and others, 1989). This optically-equivalent sphere was assumed to have the same reflecting properties as the sintered ice grains in the snow cover.

An inversion technique has been developed that is able to relate accurately the optically-equivalent grain radius in the top of the snow pack to snow reflectance in the near-infrared wavelengths (Nolin and Dozier, 1992). Earlier methods for estimating snow grain size from reflectance measurements have been qualitative (e.g. Hyvärinen and Lammasniemi, 1987; Dozier, 1989) while the method described here gives quantitative estimates of equivalent grain radius. The technique was used on measured reflectance data to retrieve estimates of optically-equivalent sphere radius.

The surface-to-volume ratio of snow depends on the actual grain size distribution, the snow bulk density, the degree of sintering of the ice grains and the liquid water content. Surface-to-volume ratio was measured by stereologic analysis on snow samples, collected in the field during the experiment. Measurements were converted to equivalent sphere sizes for comparison to snow model and inversion algorithm predictions.

Measurements used in this study were carried out at a snow study plot on Mammoth Mountain in the Sierra Nevada of California in March and April, 1989.

SIMULATION OF SNOW MICROSTRUCTURE CHANGES

A one-dimensional mass and energy balance model, SNTHERM.89 (Jordan, 1991) was used to calculate the components of the surface energy exchange, net energy budget in the near-surface snow layer, snow density and snow grain-size. The mass balance in a particular layer depends on the net vapor and liquid fluxes to the layer, which were computed by the model. Periodic snow property measurements consisted of temperature and density profiles, samples for stereological analysis were obtained concurrently and the measurements were used to initialize model runs. This model is comprehensive and can be used to simulate conditions found throughout the accumulation and ablation of a snowpack. Surface boundary conditions in SNTHERM.89 are controlled by meteorological measurements of air temperature, dew point, wind speed, precipitation and incoming and outgoing solar and infrared radiation. Components of the surface energy exchange were monitored at 30 min intervals using arrays of up-looking and down-looking hemispheric radiometers,

anemometers, air temperature sensors and relative humidity sensors.

The grain growth algorithm for dry snow is an adaptation of a function used to predict growth by sintering in metals and ceramics and found by Gow (1971) to replicate successfully grain growth observations in Antarctica.

$$\frac{\partial d}{\partial t} = \frac{g1|U_V|}{d} \tag{1}$$

where *d* is the mean grain diameter (m), *g1* is an empirical fitting parameter ($g1 = 5.010^{-7} \text{ m}^4 \text{ kg}^{-1}$), and *U_V* is the mass vapor flux ($\text{kg m}^2 \text{ s}^{-1}$), which is computed from Fick's law (Jordan, 1991).

The algorithm for grain growth in wet snow is divided depending on the saturation regime of the liquid water, pendular or funicular (Colbeck, 1982). The two functions are similar to those used for dry snow:

$$\frac{\partial d}{\partial t} = \frac{g2}{d} (\theta_1 + 0.05) \tag{2}$$

when the liquid water fraction θ_1 satisfies the condition $0.00 < \theta_1 < 0.09$ and

$$\frac{\partial d}{\partial t} = \frac{g2}{d} (0.14) \tag{3}$$

when $\theta_1 \geq 0.09$, where *g2* is an adjustable variable. Grain-growth rate increases with liquid water content up to the start of the funicular regime at $\theta_1 \geq 0.09$. An approximate fit to the data reported in Colbeck (1982, 1986) yields a value $g2 = 4.0 \times 10^{-2} \text{ m}^2 \text{ s}^{-1}$ for a liquid volume fraction $\theta_1 = 0.09$.

SNOW MICROSTRUCTURE RECOVERED FROM REFLECTANCE MEASUREMENTS

A new technique was used to recover the optical grain size from reflectance measurements (Nolin and Dozier, 1992). The basis for the inversion technique is that reflectance is sensitive to grain-size in the near-infrared spectral region. Figure 1 demonstrates the sensitivity of reflectance to

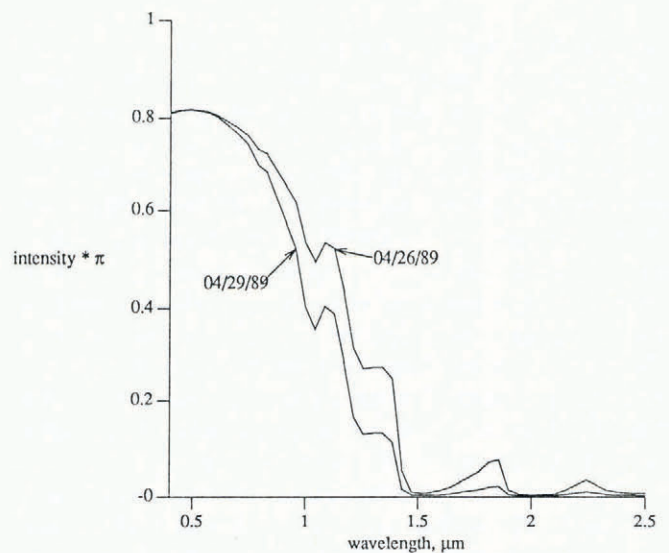


Fig. 1. Angular reflectance as a function of grain radius, calculated using a discrete-ordinate model.

grain-size at a wavelength of $1.04\ \mu\text{m}$. In this part of the spectrum ice is moderately absorbing therefore, snow with low surface-to-volume ratio (large equivalent grain radii) will have lower reflectance.

We modeled the directional reflectance using a discrete-ordinate radiative transfer model (Stamnes and others, 1988). This model differs from that of the two-stream radiative transfer modeling approach in that the discrete-ordinate model calculates the angular distribution of reflected solar radiation rather than the hemispherically-integrated value that is obtained using the two-stream approach. The ability to calculate angular reflectance is particularly important for snow because it is strongly forward-scattering, more so in the near-infrared than in the visible wavelengths (Warren, 1982); the difference between hemispherically-integrated reflectance and measured directional reflectance can be quite large depending on the solar and sensor geometries. This difference is greatest at low angles of solar incidence and when the sensor is positioned looking toward the sun at large zenith angles. Although reflectance measurements were all made at nadir viewing angles (relative to the snowpack surface), the discrete-ordinate model is preferred over the two-stream model for extending this technique for use with future sensors that would not necessarily be using nadir viewing angles—this is particularly common in the complex terrain of alpine regions.

The discrete-ordinate model takes as input values of optical thickness, single-scattering albedo, asymmetry parameter (or the coefficients of the Legendre polynomial that describes the scattering phase function), direct and diffuse incident irradiance, substrate reflectance, and solar and sensor geometries. Snowpack optical thickness, single-scattering albedo and asymmetry parameter were calculated from snow layer thickness, snow density and equivalent grain size. If the snow pack is optically semi-infinite, that is, if the substrate reflectance causes less than a 1% change in the snow cover reflectance (Dozier and others, 1989), then snow density and depth have a negligible effect on snow-cover reflectance (Bohren and Beschta, 1979) leaving grain-size as the primary parameter that influences the near-infrared reflectance of snow.

If both solar and measurement geometries are known, one can develop the mathematical transformation from optically-equivalent grain radius to angular reflectance using a least-squares fit (Nolin and Dozier, 1992). This permits the inversion from measured reflectance to grain radius. This inversion technique has been validated over a wide range of snow grain-sizes using ground reflectance measurements and stereologic analysis of snow samples.

SNOW PROPERTY AND REFLECTANCE MEASUREMENTS

The SNTHERM.89 model run was initialized with snow measurements obtained from a snow pit on 30 March 1989. The snow temperature profile was measured with an electronic probe using a thermistor for the sensor. Density measurements were determined from one litre cuts weighed in the field on an electronic top-loading balance. The measurements were replicated and repeated

at many depths to determine the density profile of the snowpack. Samples were acquired for stereology from locations in the snow layers determined to be representative from in situ stratigraphic analysis. Snow samples were prepared in the field, transported to a cold room, and sectioned for photography. Preparation of snow samples for sectioning involves filling the pore space by saturating the sample with dimethyl phthalate (Perla, 1982). Section cuts were carried out by planing the surface on a microtome, polishing with lens paper or silk, and sublimating the exposed ice profiles for a period depending on the temperature and humidity in the cold room (e.g. Perla, 1982; Davis and others, 1987). At this point, a set of photographs was taken using oblique illumination to highlight grain bond lines, which were manually counted and measured. Bond areas were estimated by assuming they are planar and circular, and the sizes were estimated from the average lengths of the bond lines (Gurland, 1958). Pits left by the ice sublimation were treated to enhance contrast by filling with finger print powder and further polishing. Photographs of the surface were then digitized and classified into ice and pore space. The volume fraction of the snow matrix is simply the ratio of the number of ice pixels to the number of pore pixels. Any liquid water in the samples is frozen and is treated as part of the ice volume.

The surface-to-volume ratio S_V is estimated by counting the intersect density of ice-air transitions N_f^h in horizontal h and vertical v directions on the section cut

$$S_V = \frac{\pi}{2} N_f^h + \left[2 - \frac{\pi}{2} \right] N_f^v. \quad (4)$$

The total area of the grains is obtained from S_V and the total area of the bonds. By assuming the grains are equal size and spherical, the grain-size can be estimated. This grain size parameter was used to initialize SNTHERM.89 and was compared at the end of the simulation to additional measurements.

From 26 to 29 April 1989 a series of snowpack spectral reflectance measurements was made using a Spectron Engineering SE-590 spectroradiometer which has usable spectral range from $0.4\ \mu\text{m}$ to $9.0\ \mu\text{m}$. A second sensor head (a prototype unit) was also used that allowed measurements of shortwave infrared reflectance out to $2.5\ \mu\text{m}$. The area sampled in the field-of-view of each instrument was roughly $90\ \text{cm}^2$. For both the visible and shortwave infrared measurements, the sensor heads were oriented perpendicular to the snow surface for nadir viewing angles. Measurement times were automatically recorded so that solar incidence angles could be calculated for each measurement. All data were collected between 0900 and 1100 h and solar zenith angles ranged from 44° to 23° . Several scans were rapidly made and then averaged for a single spectral measurement. Near-concurrent spectra were also acquired over a calibrated halon reference standard (Weidner and Hsia, 1981). The ratio of the two spectra (snow/halon) provided our estimate of the spectral reflectance. Based on the appearance of noise in the shortwave infrared spectra, we believe the measurements obtained by the prototype sensing element at a narrow band centered on $1.075\ \mu\text{m}$ were accurate, but the accuracy of the data at longer wavelengths, $1.5\ \mu\text{m}$ to $2.5\ \mu\text{m}$ was questionable.

RESULTS

The energy and mass transfer simulation was run from 30 March to 29 April 1989. Values of the model grain-size and density were obtained from the simulation times

Table 1. Equivalent grain radii from stereological measurements of snow samples collected in the field and equivalent grain radii derived from snow grain sizes simulated by SNTHERM.89

Snow depth from surface	Sphere radius from stereology	Sphere radius from simulation
	μm	μm
26 April 1989		
0-5	140	155 (depth = 1.12 cm)
5-15	161	158 (depth = 13.48 cm)
29 April 1989		
0-2	393	171 (depth = 2.0 cm)
3-7	161	171 (depth = 4.0 cm)

Table 2. Snow-grain radii values retrieved from reflectance measurements and geometrically-equivalent grain radii from stereologic analysis of concurrently-collected snow samples

SE-590 measured reflectance	Sphere radius from technique	Sphere radius from stereology
	μm	μm
26 April 1989		
0.687	150	140 (0-5 cm snow depth)
0.683	140	161 (5-15 cm snow depth)
0.684	140	
0.680	150	
0.684	140	
0.636	180	
0.653	160	
0.659	150	
mean = 0.671	mean = 151	
29 April 1989		
0.60	390	462, 323 (0-2 cm snow depth, mean = 393)
0.60	390	166, 156 (3-7 cm snow depth, mean = 161)
0.66	260	153 (7-10 cm snow depth)
0.62	340	
mean = 0.62	mean = 345	

corresponding to 1200 h on 26 April and 1200 h on 29 April. The surface-to-volume ratio of the snow was measured stereologically on these days, and the samples were acquired within minutes of 1200 h. The bond surface area was also determined from some of these samples and was used to convert the model-estimated grain-sizes to S_V . An average value of 0.5 was used to represent the fraction of grain surface area occupied by bonds or particle-to-particle contacts. The S_V value was then transformed to the geometrically equivalent sphere and in Table 1 the model-derived equivalent grain sizes are compared with the measured values.

A period of clear, warm days and cold nights from 26 to 29 April 26 caused the snowpack to change from fairly uniform, relatively small grains to a stratified snowpack with much larger melt-freeze grains in the top few millimeters of the snow. The dramatic grain growth and increase in the fraction of contact area is evident in the stereologically determined equivalent sphere size. However, the bond lines in this sample were not measured so that we could not make a reliable estimate of the equivalent sphere size, so we show the size derived from using 0.5 as the fraction of contact area.

Using the previously described inversion technique, we obtained estimates of grain-sizes that closely corresponded to those calculated by stereologic analysis of snow samples. We used reflectance values for a wavelength centered at $1.075 \mu\text{m}$, and made multiple reflectance measurements. Table 2 presents the results from both the inversion retrieval and the stereologic determination of snow grain radii for the two days.

Figure 2 shows the modeled spectral reflectance and the measurements made with the prototype sensing head in the shortwave infrared spectral region, 1.05 to $1.55 \mu\text{m}$. The measurements show reasonable values in the region centered at $1.075 \mu\text{m}$, but lack the spectral structure at longer wavelengths, which have been reported by

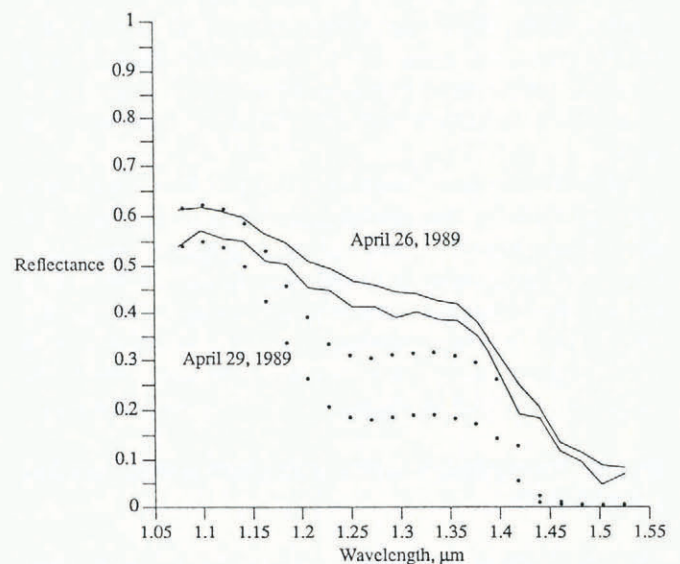


Fig. 2. Near-infrared reflectance of two snowpacks, measured (solid lines) using a modified SE-590 radiometer and calculated (dotted lines) using a discrete-ordinate model. Upper = 26 April 1989, lower = 29 April 1989.

elsewhere. We suspect the addition of intensities due to order effects at wavelengths longer than about $1.15\ \mu\text{m}$, which are evidenced by the regular signal variation, particularly in the 26 April measurements.

DISCUSSION

In this study we have compared predictions of the optically-equivalent sphere radius in the visible and near-infrared spectral regions with measurements carried out on field samples. Equivalent sphere sizes were derived from grain growth simulations by an energy and mass transfer model, but these require an estimate of the fraction of grain area occupied by particle-to-particle contacts. If this is measured we have shown that there is close agreement between the model simulations and the stereological measurements of dry snow. Equivalent sphere sizes were also estimated by inverting a model of the directional reflectance of snow. We show that these estimates show good agreement with the stereological measurements. Thus we have shown the potential to couple snow property simulations to snow reflectance models. The simulated spectral reflectance calculated for measured optical grain-sizes for the two days in this study is shown in Figure 3.

This study is limited in scope. Similar measurements are needed over a wide variety of snow types to extend the snow-modeling efforts and further validate the reflectance modeling. The study was carried out with relatively fine-grained snow with rounded grains and the same snow with a surface crust. The formation of the crust involved rapid grain growth and a large increase in bond area fraction. Further model development in this direction will attempt to formulate expressions relating snow density, grain size and thermal history to the sintering process to estimate the grain contact areas. In addition, measurements are needed on the liquid water contents retained by the surface during crust development. Measurements of the bidirectional reflectance of snow have shown features not simulated by the directional reflectance model. For example, we have observed a slight peak in reflected intensity scattered back in the direction of the solar beam, and this has been reported by Steffen (1987). Moreover the issues of absorbing contaminants needs to be addressed in both models. The algorithms in SNTherm.89 will require more development to incorporate the wavelength dependence of solar transmission and absorption in snow. This is needed to provide better characterization of the energy and mass transfer processes near the snow surface, and also to make coupling this model with reflectance models more mathematically consistent.

ACKNOWLEDGEMENTS

We are grateful for logistical support by the Mammoth/June Ski Resort. We greatly appreciate the efforts of Al Chang and Ken Brown from NASA Goddard Space Flight Center who made the spectral reflectance measurements and provided technical assistance. Dan Dawson provided a critical part of the energy balance

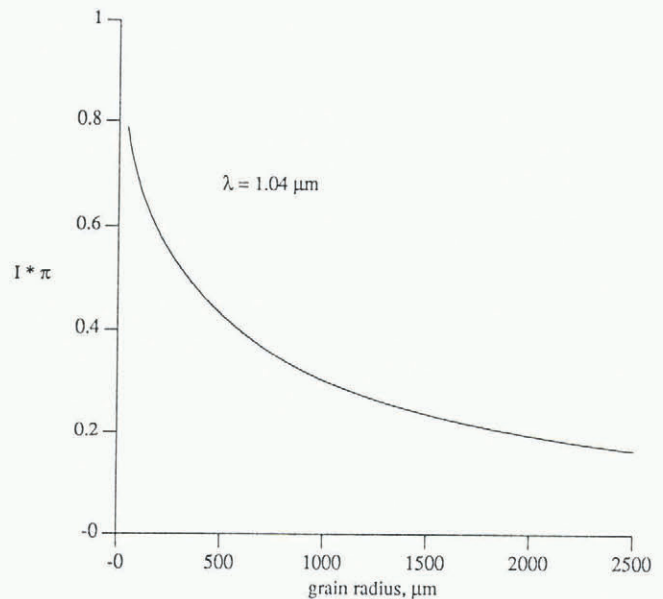


Fig. 3. Angular reflectance vs wavelength for two snowpacks, calculated using a discrete-ordinate model.

data, as well as logistical assistance. Data reduction and stereological analyses were performed at the Sierra Nevada Aquatic Research Laboratory, University of California. This work was supported by NASA Grant NAGW 1265 and by U.S. Army Corps of Engineers Project 4AT76284AT42.

REFERENCES

- Bohren, C. F. and R. L. Beschta. 1979. Snowpack albedo and snow density. *Cold Reg. Sci. Technol.*, **1**(1), 47–50.
- Colbeck, S. C. 1979. Grain clusters in wet snow. *J. Colloid Interface Sci.*, **72**(3), 371–384.
- Colbeck, S. C. 1982. An overview of seasonal snow metamorphism. *Rev. Geophys. Space Phys.*, **20**(1), 45–61.
- Colbeck, S. C. 1986. Statistics of coarsening in water-saturated snow. *Acta Metall.*, **34**, 347–352.
- Colbeck, S. C. 1989. Snow-crystal growth with varying surface temperatures and radiation penetration. *J. Glaciol.*, **35**(119), 23–29.
- Davis, R. E. 1991. Links between snowpack physics and snowpack chemistry. In Davies, T. D., M. Tranter and H. G. Jones, eds. *Seasonal snowpacks; processes of compositional change*. Berlin, etc., Springer-Verlag, 115–138.
- Davis, R. E., J. Dozier and R. Perla. 1987. Measurement of snow grain properties. In Jones, H. G. and W. J. Orville-Thomas, eds. *Seasonal snowcovers: physics, chemistry, hydrology*. Dordrecht, etc., D. Reidel Publishing Co., 63–74. (NATO ASI Ser. C 211.)
- Dozier, J. 1989. Spectral signature of alpine snow cover from the Landsat Thematic Mapper. *Remote Sensing Environ.*, **28**, 9–22.
- Dozier, J., R. E. Davis and A. Nolin. 1989. Reflectance and transmittance of snow at high spectral resolution. *IGARSS'89. 12th Canadian Symposium on Remote Sensing. Quantitative remote sensing, an economic tool for the nineties, Vancouver, Canada, July 10–14, 1989. Volume 3*, 662–664.

- Gow, A.J. 1971. Depth-time-temperature relationships of ice crystal growth in polar glaciers. *CRREL Res. Rep.* 300.
- Grenfell, T.C. and G.A. Maykut. 1977. The optical properties of ice and snow in the Arctic Basin. *J. Glaciol.*, **18**(80), 445-463.
- Gurland, J. 1958. The measurement of grain continuity in two-phase alloys. *Trans. Metall. Soc. AIME*, **202**, 452-455.
- Hyvarinen, T. and J. Lammasniemi. 1987. Infrared measurement of free-water content and grain size of snow. *Opt. Eng.*, **26**(4), 342-348.
- Jordan, R. 1991. A one-dimensional temperature model for a snow cover. *CRREL Spec. Rep.* 91-16.
- Nolin, A. and J. Dozier. In press. Estimating snow grain size using AVIRIS data. *Remote Sensing Environ.*
- Perla, R. 1982. Preparation of section planes in snow specimens. *J. Glaciol.*, **28**(98), 199-204.
- Stamnes, K., S. Tsay, W. Wiscombe and K. Jayaweera. 1988. Numerically stable algorithm for discrete-ordinate-method radiative transfer in multiple scattering and emitting layered media. *Appl. Opt.*, **27**, 2502-2509.
- Steffen, K. 1987. Bidirectional reflectance of snow at 500-600 nm. *International Association of Hydrological Sciences Publication* 166 (Symposium at Vancouver 1987 — *Large Scale Effects of Seasonal Snow Cover*), 415-425.
- Warren, S.G. 1982. Optical properties of snow. *Rev. Geophys. Space Phys.*, **20**(1), 67-89.
- Warren, S.G. and W.J. Wiscombe. 1980. A model for the spectral albedo of snow. II. Snow containing atmospheric aerosols. *J. Atmos. Sci.*, **37**(12), 2734-2745.
- Weider, V.R. and J.J. Hsia. 1981. Reflection properties of pressed polytetrafluoroethylene powder. *J. Opt. Soc. Am.*, **71**, 856-861.
- Wiscombe, W.J. and S.G. Warren. 1980. A model for the spectral albedo of snow. I. Pure snow. *J. Atmos. Sci.*, **37**(12), 2712-2733.

The accuracy of references in the text and in this list is the responsibility of the authors, to whom queries should be addressed.